PROCEEDINGS OF SCIENCE

# Jet production and the inelastic pp cross section at the LHC

**A. Grebenyuk***
*DESY, Hamburg, Germany*
*E-mail:* Anastasia.Grebenyuk@desy.de

**F. Hautmann**
*University of Oxford, Oxford, United Kingdom*
*E-mail:* hautmann@thphys.ox.ac.uk

**H. Jung**
*DESY, Hamburg, Germany,*
*Universiteit Antwerpen, Antwerpen, Belgium*
*E-mail:* hannes.jung@desy.de

**P. Katsas**
*DESY, Hamburg, Germany*
*E-mail:* panos.katsas@desy.de

**A. Knutsson**
*Universiteit Antwerpen, Antwerpen, Belgium*
*E-mail:* albert.knutsson@ua.ac.be

We suggest that, if current measurements of inclusive jet or charged particle production for central rapidities at the LHC are extended to lower transverse momenta, one could define a visible cross section sensitive to the unitarity bound set by the recent determination of the inelastic proton-proton cross section.

*XXI International Workshop on Deep-Inelastic Scattering and Related Subject -DIS2013,*
*22-26 April 2013*
*Marseilles,France*

*Speaker.

© Copyright owned by the author(s) under the terms of the Creative Commons Attribution-NonCommercial-ShareAlike Licence. 

PoS(DIS 2013)071

## 1. Introduction

In the high-energy limit the parton dynamics of the proton is driven by the growth of gluon densities at low momentum fractions $x \approx (p_T/\sqrt{s})e^{-y}$, where $p_T$ and $y$ are the jet transverse momentum and rapidity, and $\sqrt{s}$ is the center-of-mass energy. As the energy increases, the jet cross section rises, and eventually the perturbative prediction obtained from integrating the cross section over transverse momenta above a given $p_T$ is higher than the inelastic $pp$ cross section.

We suggest to measure the leading minijet or leading charged particle cross section integrated over transverse momentum in the visible phase space. At low but still perturbative transverse momenta such cross section is sensitive to the unitarity bound set by the inelastic proton-proton rate which has recently been measured at the LHC [1–3]. Such sensitivity appears within the range of acceptance of the measurement without using any extrapolation.

## 2. Integrated leading minijet cross section

First we consider the parton-level cross section at $\sqrt{s} = 8$ TeV (calculated using PYTHIA (version 6.425) [4]). Figure 1 (left) shows the estimate obtained from the $2 \to 2$ integrated cross section as a function of the minimum transverse momentum:

$$\sigma(p_{T\min}) = \int_{p_{T\min}} dp_T^2 \int_{-\infty}^{\infty} dy \frac{d^2\sigma}{dp_T^2 dy} = \int_{p_{T\min}} dp_{T\text{jet}}^2 \int_{-\infty}^{\infty} dy_{\text{jet}} \frac{d^2\sigma_{jet}}{dp_{T\text{jet}}^2 dy_{\text{jet}}}, \tag{2.1}$$

where the last expression gives an operational definition of $\sigma(p_{T\min})$ in terms of a measurable leading jet cross section. In Fig. 1 (left) we also show the cross section in the visible range by restricting the integration to the pseudorapidity region $|\eta| < 2.5$. For comparison we plot the

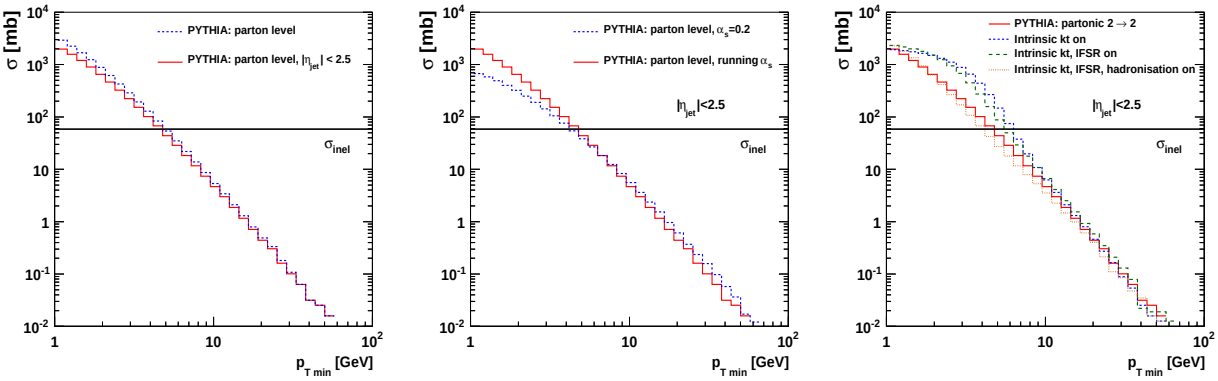


**Figure 1:** Integrated cross sections at $\sqrt{s} = 8$ TeV as a function of the minimum transverse momentum: (left) cross section compared to what can be investigated within $|\eta| < 2.5$; (middle) visible cross section in $|\eta| < 2.5$ compared to the prediction with fixed $\alpha_s = 0.2$; (right) cross section from purely partonic $2 \to 2$ process, including intrinsic $k_T$-effects, including initial and final state parton showers (IFSR) and finally hadronisation.

measurement [1–3] of the inelastic cross section, $\sigma_{\text{inel}} \sim 60$ mb as a horizontal line. One can clearly see that the partonic cross section exceeds the inelastic cross section at values of the transverse momentum at around 4 - 5 GeV even in the restricted $\eta$ range. To demonstrate the effect coming



PoS(DIS 2013)071

from infrared behaviour of the QCD coupling in Fig. 1 (middle) the cross section with $|\eta| < 2.5$ using a fixed value of $\alpha_s = 0.2$ is shown. This illustrates that the infrared behaviour of the strong coupling does not affect significantly the physical picture in the low-$p_T$ region. The rise of the cross section is essentially coming from the $1/t^2$ pole of the partonic matrix element, as explained in [5].

We then consider the cross section of jets at particle level in $|\eta| < 2.5$. In order to reconstruct the jets we use the anti-$k_T$ algorithm [6] with $R = 0.5$. The visible jet cross section is shown in Fig. 1 (right), where we show the effect of turning on successively intrinsic $k_T$, initial and final state parton showers (IFPS) and finally hadronisation (using default parameters, without allowing a taming of the cross section). The visible jet cross reaches the inelastic bound for $p_{T\min} \simeq 4$ GeV. In the region just above this value, $p_T = \mathcal{O}(10)$ GeV, effects responsible for the taming of the cross section set in. The model [5,7] provides a phenomenological modification of the low-$p_T$ behaviour of the jet cross section within a collinearly-factorised framework; the rise of the cross section is tamed at small values of $p_T$ by introducing a factor

$$\frac{\alpha_s^2(p_{T0}^2 + p_T^2)}{\alpha_s^2(p_T^2)} \frac{p_T^4}{(p_{T0}^2 + p_T^2)}, \tag{2.2}$$

where $p_{T0}$ is a parameter obtained from a fit to describe measurements of the underlying event. In Fig. 2 (left) we show the cross section based on eq.(2.2) as well as the effect of multi-parton interactions (MPI). As one can see the taming does not totally depend on MPI. The prediction of tune D6T [8] and Z2* [9] are also shown. Fig. 2 (right) we show a comparison of the jet cross

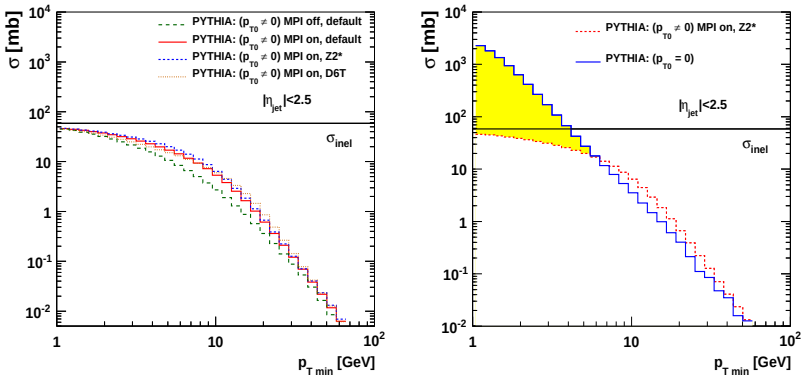


**Figure 2:** (Left) predicted cross section applying $p_{T0} \neq 0$ and MPI with different underlying event tunes of PYTHIA; (right) the solid (blue) line shows the predicted cross section applying $p_{T0} = 0$ including parton shower and hadronisation, while the dashed (red) line shows the prediction with $p_{T0} \neq 0$ including multi-parton interactions with tune Z2*.

section for $p_{T0} = 0$, including parton shower and hadronisation, with the cross section obtained from PYTHIA based on eq.(2.2).

Note that in approaches that go beyond the collinear approximation [10–17] the low-$p_T$ behaviour results from two different sources: first, the perturbative matrix elements, which are computed at finite transverse momenta $k_T$ in the initial state, have the standard collinear rise [4] at low $p_T$ for $k_T \ll p_T$, but a slower rise for $k_T \simeq p_T$ [13, 14, 16, 17]; second, the unintegrated parton densities enhance the relative weight of finite transverse momentum contributions compared



PoS(DIS 2013)071

to collinearly-ordered contributions, due to both Sudakov and Regge suppression of the low-$k_T$ region [10,11,16,17]. In the MC program CASCADE, which is based on the approximation beyond the collinear one ($k_T$-factorised framework), the unintegrated parton density function (uPDF) was modified such that it goes to zero as $k_T \to 0$, as shown in Fig. 4 (left). In Fig. 4 (right) the prediction of modified CASCADE is compared to PYTHIA applying $p_{T0} \neq 0$, showing that the cross section predicted by CASCADE also does not exceeds the inelastic cross section.

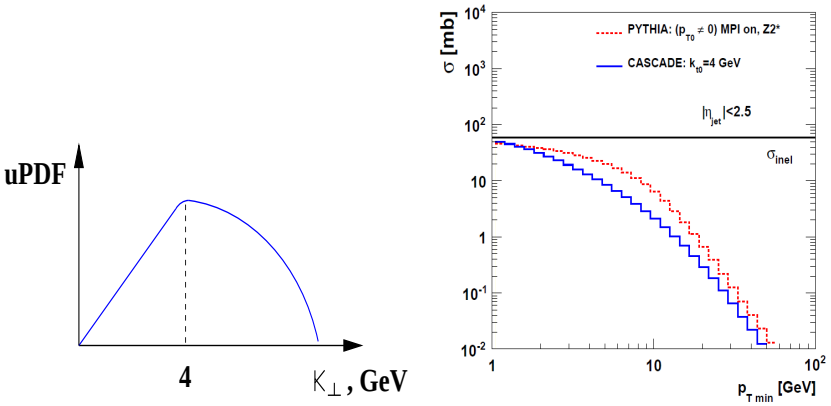


**Figure 3:** (Left) sketch showing the modification of uPDF used in CASCADE MC generator to tame the cross section; (right) visible cross section predicted by PYTHIA applying $p_{T0} \neq 0$ compared to prediction obtained by CASCADE with modified uPDF.

## 3. Integrated leading charged particle distribution

With the same physics motivation as for minijets one can consider the integrated leading charged particle cross section. Such distribution obtained by PYTHIA is shown in Fig. 4 (left). The

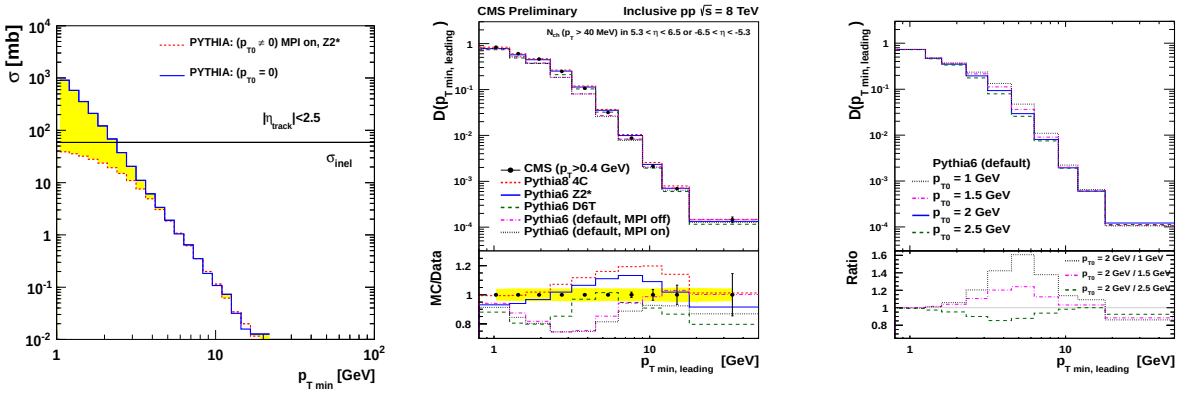


**Figure 4:** (Left) the solid (blue) line shows the predicted integrated leading charged particle cross section applying $p_{T0} = 0$, while the dashed (red) line shows the prediction with $p_{T0} \neq 0$ including multi-parton interactions with tune Z2*; (middle) measured normalised integrated $p_T$-distribution of the leading charged particle together with predictions from different PYTHIA6 and PYTHIA8 tunes; (right) predicted normalised integrated $p_T$-distribution of the leading charged particle with default tune but different values of $p_{T0}$.

$p_T$ distribution is softer compared to the minijets (see Fig. 2 (right)) and the cross section reaches



PoS(DIS 2013)071

the inelastic bound for $p_{T\min} \simeq 1.5$ GeV. It has been studied that this strongly depends on the cone radius for the minijets, with $R = 0.1$ a distribution similar to the charged particles is observed. The recent measurements of this observable has been presented by the CMS Collaboration [18]. The event normalised distribution $D(p_{T\min,\text{leading}})$, defined as

$$D(p_{T\min,\text{leading}}) = \frac{1}{N}\int_{p_{T\min,\text{leading}}} dp_{T\min,\text{leading}} \left(\frac{dn}{p_{T\min,\text{leading}}}\right), \tag{3.1}$$

where $N$ is the number of event that fulfils the required event and charged particle selection, is shown in Fig. 4 (middle). The data are compared to predictions obtained from PYTHIA8 4C, PYTHIA6 Z2*, PYTHIA6 D6T and PYTHIA default tune with and without multi-parton interactions. For both distributions, we observe that all theoretical predictions fail to describe the shape of the data. The effect of multi-parton interactions is shown to have a small impact. The effect of regularisation parameter $p_{T0}$ is shown in Fig. 4 (right) by varying $p_{T0}$ value in PYTHIA.

## References


[1] ATLAS, G. Aadet al., Nature Commun.2, 463 (2011), arXiv:1104.0326.

[2] CMS Collaboration, Measurement of the inelastic pp cross section at sqrts = 7 TeV, CMS-PAS-QCD-11-002 https://cdsweb.cern.ch/record/1433413?ln=en, 2012.

[3] CMS Collaboration, Inelastic pp cross section at 7 TeV, CMS-PAS-FWD-11-001 https://cdsweb.cern.ch/record/1373466?ln=en, 2011.

[4] T. Sjöstrand, S. Mrenna, and P. Skands, JHEP 05, 026 (2006), arXiv:hep-ph/0603175.

[5] T. Söstrand and P. Skands, JHEP 03, 053 (2004), arXiv:hep-ph/0402078.

[6] M. Cacciari, G. P. Salam, and G. Soyez, JHEP 04, 063 (2008), arXiv:0802.1189.

[7] T. Sjöstrand and M. van Zijl, Phys. Rev. D36, 2019 (1987).

[8] R. Field, Studying the underlying event at CDF and the LHC, in *Multiple partonic interactions at the LHC. Proceedings, 1st International Workshop, MPI'08, Perugia, Italy, October 27-31, 2008*, edited by P. Bartalini and L. Fanó, pp. 12-31, 2010, arXiv:1003.4220.

[9] R. Field, (2010), arXiv:1010.3558.

[10] G. Gustafson, L. Lönnblad, and G. Miu, Phys.Rev. D67, 034020 (2003), arXiv:hep-ph/0209186.

[11] G. Gustafson, L. Lönnblad, and G. Miu, JHEP 0209, 005 (2002), arXiv:hep-ph/0206195.

[12] G. Gustafson and G. Miu, Phys.Rev. D63, 034004 (2001), arXiv:hep-ph/0002278.

[13] M. Deak, F. Hautmann, H. Jung, and K. Kutak, JHEP 09, 121 (2009), arXiv:0908.0538.

[14] M. Deak, F. Hautmann, H. Jung, and K. Kutak, Forward-Central Jet Correlations at the Large Hadron Collider, 2010, arXiv:1012.6037.

[15] F. Hautmann and H. Jung, JHEP 10, 113 (2008), arXiv:0805.1049.

[16] F. Hautmann and H. Jung, Nucl.Phys.Proc.Suppl.184, 64 (2008), arXiv:0712.0568.

[17] F. Hautmann, Acta Phys.Polon. B40, 2139 (2009).

[18] CMS Collaboration, CMS-PAS-FSQ-12-026, "Inclusive hadron production in p-p at 8 TeV".


PoS(DIS 2013)071